Stereochemical Effect of *Trans*/*Cis* Isomers on the Aqueous Solution Properties of Acid-Labile Thermoresponsive Polymers

Xiaonan Huang, Fusheng Du,* Dehai Liang, Shrong-Shi Lin, and Zichen Li*

Beijing National Laboratory for Molecular Sciences, Key Laboratory of Polymer Chemistry and Physics of Ministry of Education, College of Chemistry & Molecular Engineering, Peking University, Beijing 100871, P. R. China

Received April 8, 2008; Revised Manuscript Received May 29, 2008

ABSTRACT: Two acid-labile, thermoresponsive poly(methacrylamide)s with the pendant cyclic orthoester moieties of *trans* and *cis* configurations, P*t*NEM and P*c*NEM, were synthesized via free radical polymerization of the corresponding *trans* and *cis* isomers of *N*-(2-ethoxy-1,3-dioxan-5-yl)methacrylamide (NEM). The thermally induced phase transition/separation behaviors of both polymers as well as the aqueous solution properties below and above their phase transition temperatures were investigated by means of turbidimetry, DSC, ^{1}H NMR, microscopy, fluorescence probe, and dynamic light scattering. Both P*t*NEM and P*c*NEM showed aggregation behaviors below their respective LCSTs, and the former formed more hydrophobic microdomains which had greater capability to solvate pyrene molecules compared with P*c*NEM. These two polymers exhibited thermally induced sensitive and reversible phase transitions in aqueous solution. P*t*NEM showed a little lower cloud point but much greater phase transition enthalpy compared to P*c*NEM. The results of DSC, ^{1}H NMR, and microscopy measurements revealed that P*c*NEM exhibited a liquid−liquid phase separation while P*t*NEM likely underwent a liquid−solid transition. Furthermore, the pH-dependent hydrolyses of both polymers were studied by the ^{1}H NMR and turbidimetric approaches. The results indicated that both P*t*NEM and P*c*NEM showed acid-triggered hydrolysis behaviors, and the hydrolysis products were affected by the configurations of the pendant cyclic groups. On the basis of these results, we can conclude that the stereochemical structures of the pendant cyclic orthoester groups in these poly(methacrylamide)s greatly affect their aqueous solution properties as well as their hydrolysis behaviors.

Introduction

Stimuli-responsive polymers,[1] especially thermoresponsive polymers which display lower critical solution temperature (LCST) in aqueous solution, have been extensively studied for their potential applications in various fields such as catalysis, drug and gene delivery, separation and purification of biomolecules, cell culture, biosensors, etc.[2] Besides the classical synthetic polymers with LCSTs such as poly(*N*-substituted acrylamide)s, poly(*N*-vinylamide)s, poly(vinyl ether)s, and poly(organophosphazene),[1] biodegradable, recombinant artificial elastin-like polypeptides, hyperbranched and dendritic polymers with LCSTs have also been developed.[3] The phase transition temperature of a thermoresponsive polymer with LCST largely depends on the hydrophilic/hydrophobic balance in the polymer.[1b,4] In general, homopolymers with various amphiphilicities in the monomer units may show different LCSTs. However, it is difficult to precisely control the LCST by designing a specific monomeric structure. Another facile approach for tuning LCST is the copolymerization of monomers with different hydrophilic/hydrophobic natures.[4b,5] The comonomer structure, composition, and sequence distribution of the comonomer units in the copolymer have been confirmed to affect the LCSTs of the copolymers.[6] Recently, much effort has been directed to clarify the effects of other parameters including molecular weight and its distribution,[7] chain-end group,[8] topology or molecular shape,[9] additives,[10] etc., on the phase transition behaviors of thermoresponsive polymers. While most of these reports are related to the constitutional factors that affect LCST, little attention was paid to the stereochemical effect of molecular parameters on the phase transition properties of polymers. Aoki et al. found that a chiral polymer was quite different in thermosensitive properties compared with the optically inactive one.[11] It was also reported that the chain tacticities of thermoresponsive polymers affected their thermal behavior in aqueous solution.[12]

Intelligent polymers capable of responding to both pH and temperature have been widely investigated because of their great potentials for biomedical and pharmaceutical uses.[13] Most of these doubly responsive polymers, however, contain titratable groups such as carboxylic or amino groups.[14] Recently, we reported a new type of acid-labile, thermoresponsive polymers with pendant cyclic orthoester or acetal groups. The water-insoluble polymers above their respective LCSTs dissolved gradually with the hydrolysis of the pendant groups.[15] In contrast to other hydrolyzable thermoresponsive polymers that are susceptible to hydrolysis under the neutral or basic environments,[16] our polymers are relatively stable in the neutral or basic media but labile in low-pH solutions. This acid-labile feature makes these new polymers, especially the orthoester-containing ones, potential as candidates for the drug delivery systems that remain stable in blood but are capable of releasing their payload at mildly acidic sites, such as in tumor tissues or endosomes.[17] In the previous paper, the (co)polymers with the pendant orthoester groups were prepared from the monomer mixtures of *trans* (45%) and *cis* (55%) isomers.[15a] Fortunately, we separated the *trans* and *cis* isomers of *N*-(2-ethoxy-1,3-dioxan-5-yl)methacrylamide (NEM) and prepared their homopolymers (P*t*NEM and P*c*NEM) via radical polymerization (Scheme 1). We found that the two polymers displayed quite different thermoresponsive properties as well as hydrolysis behaviors in the aqueous solutions. In this work, we use different approaches to study the aqueous solution properties of P*t*NEM and P*c*NEM and report some interesting results, including the aggregation phenomenon below the LCSTs and the thermally induced phase transition behaviors. To our best knowledge, this is the first paper that reports the stereochemical effect of *trans* and *cis* configurations of the pendant groups on the solution properties of thermoresponsive polymers.

* Corresponding authors: e-mail fsdu@pku.edu.cn, zcli@pku.edu.cn; Tel 86-10-62757155; Fax 86-10-62751708.

10.1021/ma800783v CCC: $40.75
Published on Web 06/21/2008

Scheme 1. Synthetic Routes of *trans*-NEM, *cis*-NEM, and Their Polymers[a]

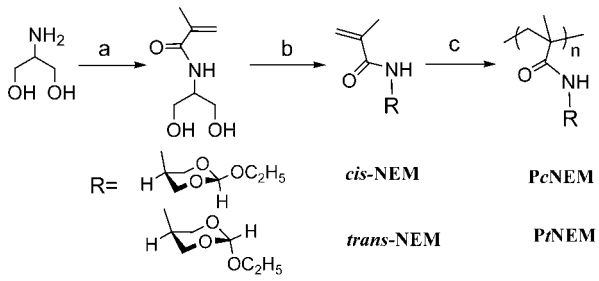

[a] Conditions: (a) methacryloyl chloride, 10% Na_2CO_3 aqueous solution, 0−5 °C, 5 h; (b) triethyl orthoformate, $TsOH \cdot H_2O$, rt, 2 h; (c) AIBN, 60 °C, 24 h in dioxane.

Experimental Section

Materials. 2-Amino-1,3-propanediol (Hua Qing Run De Co., Beijing, China), triethyl orthoformate, and D_2O (Acros) were used as received. 1,4-Dioxane and tetrahydrofuran (THF) were distilled over sodium prior to use. 2,2′-Azobis(isobutyronitrile) (AIBN) was recrystallized twice from methanol. $CDCl_3$ (Acros) was treated with anhydrous Na_2CO_3 before NMR measurements for detecting the orthoester-containing samples. Pyrene (Acros) was recrystallized from ethanol twice. Methacryloyl chloride was synthesized from methacrylic acid and benzoyl chloride according to a modified method from the literature.[18] *N*-(1,3-Dihydroxypropan-2-yl)methacrylamide was synthesized by the same procedure as reported previously.[15] Other solvents and reagents were purchased from Beijing Chemical Reagent Co. and used as received.

Synthesis of *trans*- and *cis*-NEM. A mixture of *trans*-NEM and *cis*-NEM was prepared according to the previous procedure.[15a] Briefly, *N*-(1,3-dihydroxypropan-2-yl)methacrylamide (5.0 g, 31 mmol), *p*-toluensulfonic acid monohydrate (59 mg, 3.1 mmol), and triethyl orthoformate (3.4 mL, 31 mmol) were dissolved in 100 mL of distilled THF, and the reaction mixture was stirred at room temperature for 4 h. After removing the solvent under reduced pressure, the residue was prepurified through an Al_2O_3 column using ethyl acetate as the eluent. The separation of the *cis* isomer from the *trans* isomer was achieved by repeated chromatography through an Al_2O_3 column with hexane/ethyl acetate (5:2 v/v) as the eluent, followed by recrystallization in hexane/THF (5:1). The resultant pure *cis*-NEM and *trans*-NEM were in the state of white crystals. *trans*-NEM: ^{1}H NMR (TMS, $CDCl_3$, ppm, Figure S1): 6.73 (s, 1H, −N*H*CO−), 5.75 (s, 1H, CH_2═C−), 5.43 (s, 1H, C*H*O_3), 5.36 (s, 1H, CH_2═C−), 4.38 (d, 2H, N−CH(CH_2)$_2$, axial), 4.0 (m, 1H, N−C*H*(CH_2)$_2$), 3.63 (d, 2H, N−CH(CH_2)$_2$, equatorial), 3.58 (q, 2H, −OCH_2CH_3), 1.98 (s, 3H, C═C(CH_3)), 1.26 (t, 3H, −OCH_2CH_3). ^{13}C NMR ($CDCl_3$, ppm, Figure S1): 168.0 (−*C*═O), 139.8 (CH_2═*C*−), 120.1 (*C*H_2═C−), 107.4 (−*C*HO_3), 62.0 (N−CH(*C*H_2)$_2$), 61.4 (−O*C*H_2CH_3), 43.6 (N−*C*H(CH_2)$_2$), 18.5 (C═C(*C*H_3)), 14.8 (−OCH_2*C*H_3). FT-IR (KBr, cm^{-1}): 3284, 2977, 2862, 1651, 1612, 1533, 1380, 1212, 1151, 1121. MS: 214 (M − 1)$^+$. Elemental analysis: Calcd C% 55.80, N% 7.96, H% 6.51. Found C% 55.70, N% 7.99, H% 6.37; mp 74.4−76.5 °C. *cis*-NEM: ^{1}H NMR (TMS,$CDCl_3$, ppm, Figure S2): 6.62 (s, 1H, −N*H*CO−), 5.75 (s, 1H, CH_2═C−), 5.38 (s, 1H, CH_2═C−), 5.26 (s, 1H, C*H*O_3), 4.03 (s, 4H, N−CH(CH_2)$_2$), 4.01 (m, 1H, N−C*H*(CH_2)$_2$), 3.78 (q, 2H, −OCH_2CH_3), 1.99 (s, 3H, C═C(CH_3)), 1.28 (t, 3H, −OCH_2-CH_3). ^{13}C NMR ($CDCl_3$, ppm, Figure S2): 167.8 (−*C*═O), 139.3 (CH_2═*C*−), 121.0 (*C*H_2═C−), 112.1 (−*C*HO_3), 67.6 (N−CH-(*C*H_2)$_2$), 61.8 (−O*C*H_2CH_3), 42.6 (N−*C*H(CH_2)$_2$), 18.3 (C═C-(*C*H_3)), 14.7 (−OCH_2*C*H_3). FT-IR (KBr, cm^{-1}): 3306, 2974, 2886, 1656, 1622, 1540, 1153, 1078, 1051, 1016. MS: 214 (M − 1)$^+$. Elemental analysis: Calcd C% 55.80, N% 7.96, H% 6.51. Found C% 55.73, N% 8.03, H% 6.41; mp 70.8−71.2 °C.

Polymerization. *trans*-NEM or *cis*-NEM and AIBN (1.0 mol % relative to monomers) were weighted into a polymerization tube, to which the dried dioxane was added to dissolve the monomer and initiator. The final concentration of the monomer was ca. 0.10 g/mL. After three cycles of freeze−pump−thaw to thoroughly remove oxygen, the tube was sealed in vacuo, and the polymerization was carried out at 60 °C for 24 h. The polymers were precipitated from diethyl ether twice, collected by filtration, and dried in vacuo to afford white powders. The molecular weights and polydispersity indices of the polymers were determined by gel permeation chromatography (GPC).

GPC Measurement. GPC measurements were performed on an equipment consisting of a Waters 1525 binary HPLC pump, a Waters 2414 refractive index detector, and three Waters Styragel columns (HT2, HT3, and HT4). Temperature of the columns was set at 35 °C in a thermostat, and THF was used as the eluent with a flow rate of 1.0 mL/min. The concentration of the injected polymer solutions was ca. 10 mg/mL. A family of narrow dispersed polystyrenes was used as the standards and a Millennium 32 software was applied to calculate the molecular weight and polydispersity index.

NMR Spectroscopy. ^{1}H NMR spectra of the monomers and polymers in $CDCl_3$ were recorded on a Bruker 400 MHz spectrometer using tetramethylsilane (TMS) as the internal reference. ^{1}H NMR spectra of the polymers in the deuterated buffers and ^{13}C NMR spectra of the monomers in $CDCl_3$ were recorded on a Varian Mercury Plus 300 MHz NMR spectrometer. For the ^{1}H NMR measurements of varying temperature or time-dependent hydrolysis in the deuterated buffers, the Varian Mercury Plu 300 MHz NMR spectrometer was applied with maleic acid as an internal standard.

Transmittance Measurement. The transmittance of the polymer solutions in 10 mM phosphate buffer (pH 8.4) was measured at 500 nm through a 1 cm quartz cell on a Shimadzu 2101 UV−vis spectrometer which was equipped with a water-jacketed cell holder and a circulating water bath (Shimazu TB-85). Polymer-free 10 mM phosphate buffer was used as a reference. The temperatures of the polymer solutions were manually tuned at a heating or cooling rate of ca. 1 °C/min and detected by a digital internal temperature probe. Cloud point (CP) was defined as the inflection point of the transmittance vs temperature curve which was determined by the maximum in the first derivative. The phosphate buffer of pH 8.4 was used in order to avoid the hydrolysis of the orthoester groups during the measurements, except for the pH-dependent hydrolysis experiments.

Differential Scanning Calorimetry (DSC). DSC measurements were carried out on TA Instruments DSC Q100. Polymer solutions in the 10 mM phosphate buffer (10 μL, 4 wt %) were sealed in aluminum pans in order to avoid water evaporation. An aluminum pan with the same buffer (10 μL) without polymer was used as the reference. A scanning rate of 1.0 °C/min was used for both heating and cooling processes between −5 and 45 °C. The phase transition temperature (T_{max}) was defined as the maximum of the endothermic peak upon heating up or the exothermic peak upon cooling down. The transition enthalpy (ΔH) was determined from the endothermic peak area and calibrated with an indium standard.

Fluorescence Measurement. 100 μL of pyrene in THF solution (1.0×10^{-3} mol/L) was added into a 100 mL volumetric flask, and the solvent was evaporated under a nitrogen flow. Phosphate buffer (100 mL, 10 mM) was then added, and the obtained solution was equilibrated for 2 days at ambient temperature. This stock solution of pyrene was used to prepare the P*t*NEM and P*c*NEM aqueous solutions with various concentrations at 4 °C. The polymer solutions were equilibrated for 2 days at 4 °C in a refrigerator prior to the measurements. The final concentration of pyrene in all of the polymer solutions was 1.0×10^{-6} mol/L unless otherwise indicated. A Hitachi F-4500 fluorescence spectrometer was used for the fluorescence measurements. The excitation and emission slit widths of the fluorometer were set at 5.0 and 2.5 nm, respectively. The excitation wavelength was set up at 339 nm, and the emission spectra were recorded from 360 to 580 nm at a scanning rate of 240 nm/min. I_1/I_3 was defined as the intensity ratio of the first (ca. 375 nm) to the third (ca. 385 nm) bands in the emission spectrum. I_e/I_m was defined as the ratio of the excimer intensity (480 nm) to the monomer intensity (the averaged value

Table 1. Characterizations of P*t*NEM and P*c*NEM and Their Aqueous Solution Properties

	M_n[a] ($\times 10^4$)	M_w[a] ($\times 10^4$)	PDI[a]	CP[b] (°C) 0.1 wt %	CP[b] (°C) 0.5 wt %	T_{max}[c] (°C)	ΔH[d] (kJ/mol)	cac[e] (mg/mL)
P*t*NEM	3.3	5.5	1.7	18.8	17.8	17.6 (16.3)	6.1	0.15
P*c*NEM	2.9	5.2	1.8	21.9	20.0	20.8 (19.5)	1.3	0.54

[a] Determined by GPC with THF as an eluent and monodisperse polystyrenes as the standards. [b] Defined as the inflection point of the transmittance vs temperature curve, in pH 8.4 phosphate buffer, heating rate: ca. 1.0 °C/min. [c] Defined as the maximum of the endothermic or exothermic peak, 4 wt % in pH 8.4 phosphate buffer, heating/cooling rate: 1.0 °C/min. The values in the parentheses are for the cooling process. [d] Calorimetric enthalpy in kJ/mol per repeating units (heating process). [e] Measured by fluorescence method.

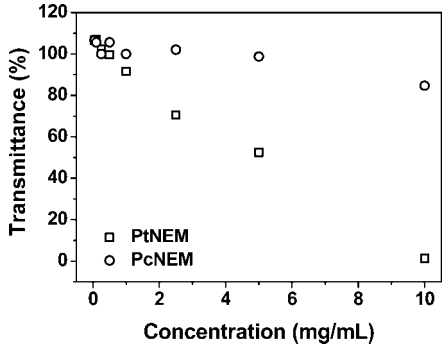

Figure 1. Transmittance values of P*t*NEM and P*c*NEM solutions in 10 mM pH 8.4 phosphate buffer at various concentrations. $\lambda = 500$ nm, 10 °C.

of I_1 and I_3). Because the polymer solutions were turbid at higher polymer concentrations (below and above their LCSTs), light scattering of the aggregate particles drastically influenced the emission spectra, especially for the monomer emission bands. In order to reduce the magnitude of this influence, the intensities of the first (I_1) and third (I_3) bands were subtracted by the intensity at 362 nm for calculating the ratio of I_1/I_3 or I_e/I_m.

pH-Dependent Hydrolysis. For the hydrolyses of P*t*NEM and P*c*NEM monitored by the turbidimetric method, each of the polymers was dissolved in a cold 10 mM pH 8.4 phosphate buffer (1.0 mg/mL). After being maintained at 37 °C for 10 min, the transmittance of the solution was 0% using the polymer-free phosphate buffer as the reference (100% transmittance). Then, the polymer solution was adjusted to pH 4.0 by the addition of 5.0 M pH 4.0 acetate buffer (0 time point), and the transmittance of the solution was measured against time at 37 °C. For hydrolyses at other pH values, different concentrated acetate buffer with various pHs (4.6, 5.0, 5.4) were used. For the hydrolyses at pD ca. 5.0 monitored by NMR spectrometry, the polymer solutions at pD 8.4 were first maintained at 37 °C for 15 min and the ^{1}H NMR spectra were measured, which were used as those at the 0 time point. After the addition of 5.0 M acetate buffer (pD 5.0), the polymer solutions were mixed quickly and maintained at 37 °C, and the ^{1}H NMR spectra were recorded at specific time points.

Results and Discussion

The mixture of *trans* and *cis* isomers of NEM was prepared according to the previous procedure; pure *trans*-NEM and *cis*-NEM were obtained after repeating column chromatography.[15a] Their configurations were confirmed by single-crystal X-ray diffraction measurements (Figures S3 and S4). The homopolymers, P*t*NEM and P*c*NEM, were then prepared by conventional free radical polymerization (Figure S5). Both polymers have similar molecular weights and polydispersities, which make it proper to compare their aqueous solution properties (Table 1).

Aggregation Behaviors below LCST. Both P*t*NEM and P*c*NEM are water-soluble at low temperature (below 17 °C), but their solution properties are strongly dependent on the polymer concentration. Figure 1 shows the plots of transmittance vs concentration of the polymers in 10 mM phosphate buffer (pH 8.4) at 10 °C. For P*t*NEM, the solution was visually clear

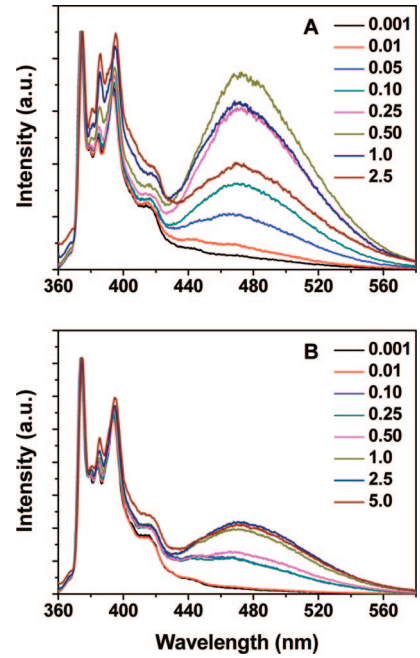

Figure 2. Emission spectra of pyrene in the P*t*NEM (A) and P*c*NEM (B) solutions (10 mM pH 8.4 phosphate buffer) at various polymer concentrations (mg/mL). $\lambda_{ex} = 339$ nm, 10 °C.

below 1.0 mg/mL, beyond which the transmittance of the solutions decreased gradually with increasing polymer concentration, approaching a value of ca. 2% at 10 mg/mL. In the case of P*c*NEM, the solutions remained completely transparent below 5.0 mg/mL and became a little cloudy at 10 mg/mL. These observations indicated that some colloidal aggregates were formed even below the LCSTs of the polymers. These colloidal solutions were stable without observable precipitates for at least 72 h at 5 °C. The presence of the colloidal aggregates in the cold polymer solutions was proved by the dynamic light scattering results (Figure S6). Bimodal size distributions were clearly observed for both polymer solutions at a low concentration of 0.10 mg/mL (10 °C). Besides the small particles with an apparent hydrodynamic radius (R_h) (<10 nm) that should represent the coiled polymer chains, there were the coexisted larger aggregates with radii of ca. 60 nm for P*c*NEM and ca. 50 nm for P*t*NEM, respectively, indicating that aggregation occurred even at low concentrations where the polymer solutions were visually transparent.

The aggregation behaviors of the polymers were further studied by the fluorescence approach using pyrene (Py) as a probe. It is well-known that the vibronic band structure of the emission spectrum of Py is sensitive to the polarity of a microenvironment in which it is dispersed. The intensity ratio (I_1/I_3) of the first (0,0) to the third (0,2) bands decreases as Py is transferred from a polar into a less polar microdomain.[19] Figure 2 shows the emission spectra of pyrene in P*t*NEM and P*c*NEM in 10 mM phosphate buffer solutions at different polymer concentrations. The spectra were normalized at the first band. It can be seen that in both polymer solutions the ratio of

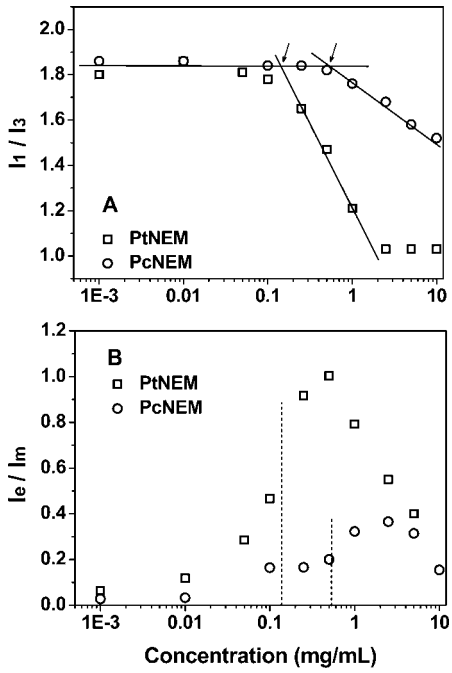

Figure 3. Dependence of I_1/I_3 (A) or I_e/I_m (B) ratio of pyrene on the polymer concentration of P*t*NEM and P*c*NEM in 10 mM pH 8.4 phosphate buffer at 10 °C.

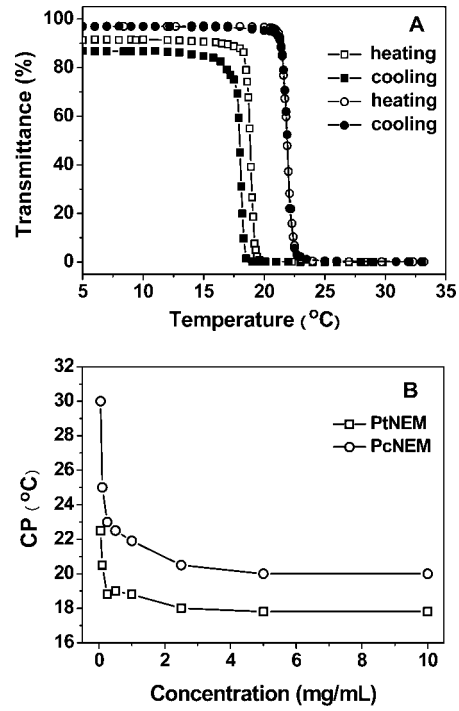

Figure 4. (A) Transmittance vs temperature plots of P*t*NEM (square) and P*c*NEM (circle) in 10 mM pH 8.4 phosphate buffer (1.0 mg/mL) in a heating and cooling cycle. (B) Dependence of the cloud points of P*t*NEM and P*c*NEM aqueous solutions at various concentrations. λ = 500 nm; heating/cooling rate: ca. 1.0 °C/min.

I_1/I_3 remained almost constant at lower polymer concentrations and decreased gradually with further increasing the concentration, indicating that Py was partitioned into a less polar environment. The critical aggregation concentrations (cac), estimated from the plots of I_1/I_3 ratio vs polymer concentration, were 0.15 mg/mL for P*t*NEM and 0.54 mg/mL for P*c*NEM (Table 1 and Figure 3A). For P*t*NEM, the ratio of I_1/I_3 reached a value of 1.04 at the concentration of 2.5 mg/mL, beyond which leveled off. This value of I_1/I_3 is close to that for Py solubilized in 1-butanol[19a] or in SDS aqueous solution.[20] In the case of P*c*NEM, the ratio of I_1/I_3 declined only to 1.53 even at a higher polymer concentration, 10 mg/mL. These results indicate that the microdomains formed by the aggregation of P*c*NEM are much more polar than that of P*t*NEM.

From Figure 2, it can also be seen that a broad featureless peak centered at ca. 475 nm, characteristic of the excimer emission of Py, was observed at higher polymer concentrations. The relative intensity of the excimer to monomer emission, depicted as I_e/I_m, was dependent upon the polymer concentration (Figure 3B). For P*t*NEM, in the range of low concentrations ($\leq$0.01 mg/mL), the excimer emission was very weak. As the polymer concentration was raised, the value of I_e/I_m increased up to a maximum somewhat above the cac, followed by a monotonic decrease in I_e/I_m with further increasing the polymer concentration. A similar trend for P*c*NEM was observed but with the lower values of I_e/I_m compared with that of P*t*NEM. These results can be attributed to the distribution of Py molecules between the aggregated microdomains and the bulk water phase. At very low polymer concentrations, there was little microdomain that can solubilize Py and most of the Py molecules were partitioned in the bulk water; as a result, no or weak excimer emission can be observed. With increasing the polymer concentration, the amount of the less polar microdomains that can trap Py molecules increased, resulting in high local Py concentration and the subsequent strong excimer emission. The largest value of I_e/I_m for an individual polymer was obtained at a specific concentration where all of the Py molecules were partitioned into the microdomains. Beyond this value, further increase in the polymer concentration would dilute Py molecules in the microdomains, thus decreasing the probability of excimer formation. A similar phenomenon was also reported for Py in the aqueous solutions of some amphiphilic copolymers[21] and can be well explained by the model for Py in the micellar solutions of small molecule surfactants as proposed by Tilton et al.[22] By comparing the aforementioned fluorescence results, we can conclude that P*t*NEM shows a higher tendency to form more hydrophobic microdomains which possess greater capability to solvate Py molecules compared to its counterpart, P*c*NEM.

In order to better understand the excimer formation mechanism, the excitation spectra of Py in P*t*NEM and P*c*NEM solutions were recorded by monitoring the monomer (390 nm) and the excimer (480 nm) emission bands, respectively (Figures S7 and S8). For either of the polymers at the lower concentrations, the excitation spectrum of the excimer was red-shifted by ca. 2.5 nm compared to that of the monomer, indicating that the excimer originated from the preformed pyrene dimers or higher aggregates that existed prior to excitation, i.e., static excimer.[23] However, the extent of the red shift became smaller at higher polymer concentrations. For P*t*NEM at 5.0 mg/mL, the excitation spectra of both monomer and excimer were almost identical. It may indicate that the dynamic excimers formed via the classic Birks mechanism, i.e., from an excited Py and a second Py in its ground state in a diffusion-controlled way, dominated the excimer emission.[19b] These results are rationalized in fact that at the higher polymer concentrations the Py molecules trapped in the microdomains were apart too "far" to form ground-state dimers or aggregates but close enough to produce the dynamic excimers.

Thermally Induced Phase Transitions. As reported previously for PNEM prepared from the mixture of *trans* and *cis* isomers,[15a] both P*t*NEM and P*c*NEM showed the thermally induced phase transition properties which were first evaluated by the turbidimetric method. Figure 4A shows the transmittance vs temperature plots of P*t*NEM and P*c*NEM in 10 mM pH 8.4 phosphate buffer (1.0 mg/mL) during a heating and a cooling

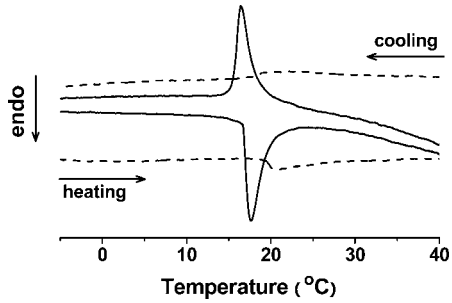

Figure 5. DSC thermograms of P*t*NEM (solid line) and P*c*NEM (dashed line) in 10 mM pH 8.4 phosphate buffer (40 mg/mL) during a heating and cooling cycle with a heating/cooling rate of 1.0 °C/min.

process. It can be seen that both polymer solutions exhibited the highly sensitive and reversible phase transitions at 18.8 °C for P*t*NEM and 21.9 °C for P*c*NEM, respectively. Upon cooling, only little hysteresis (0.9 °C) was observed for P*t*NEM. Further experiments revealed that the thermally induced phase transitions of the polymer solutions were reproducible, at least for the first three heating and cooling cycles. Compared with the previously reported CP (22.5 °C) of PNEM from *trans* (45%) and *cis* (55%) isomers, the CPs of both P*t*NEM and P*c*NEM were little bit lower.[15a] Considering the relatively higher molecular weight of the present polymers, this is reasonable. Figure 4B shows the concentration dependency of the cloud points (CPs) of P*t*NEM and P*c*NEM aqueous solutions. It is seen that both polymers demonstrated the same trends in the polymer concentration range of 0.05−10 mg/mL. The CPs initially decreased significantly with increasing the concentration and then became constant above a concentration of 2.5 mg/mL for P*t*NEM and 5.0 mg/mL for P*c*NEM. Similar observations were reported for other thermosensitive polymers, which can be attributed to the fact that the high polymer concentrations would macroscopically favor the flocculation of the primary aggregates.[24]

To obtain a better insight of the phase transition behaviors of P*t*NEM and P*c*NEM in the aqueous solutions, DSC, ^{1}H NMR, and fluorescence measurements were performed. Figure 5 shows the DSC thermograms of the polymer solutions at a 4 wt % concentration in one heating−cooling cycle. Upon heating, P*t*NEM and P*c*NEM showed the endothermic peaks with the maxima (T_{max}) at 17.6 and 20.8 °C, respectively, which were consistent with their CPs at higher polymer concentrations (Table 1). In the cooling process, the exothermic peaks were observed for both the polymers with the transition temperatures of ca. 1.3 °C lower than those in the heating process, indicating a clear hysteresis for the polymers. A similar phenomenon was also reported for poly(*N*-isopropylacrylamide) (PNIPAM), which was attributed to the formation of intra- and interchain hydrogen bonds between the amide groups (⟩C═O···H−*N*⟨) as well as the chain entanglement in the polymer aggregates.[25]

Furthermore, there was a marked difference between the transition enthalpies (ΔH) of P*t*NEM and P*c*NEM. In the heating process, ΔH of P*t*NEM aqueous solution was 6.1 kJ/mol per repeating units, comparable to that of PNIPAM (ca. 5−8 kJ/mol) with a typical coil−globule phase transition.[2f,25b] However, P*c*NEM had a much smaller ΔH (1.3 kJ/mol), suggesting the incomplete dehydration and more solvated polymer chains even above its CP. This difference in the hydration states of the polymers above their CPs was also demonstrated by their temperature-dependent ^{1}H NMR spectra (Figure 6). Below their CPs the polymer chains were well solvated and the proton signals of the polymers were clearly observed. For P*t*NEM, the signal intensities were drastically reduced around its CP with increasing the temperature. At 30 °C, ca. 12 °C above its CP, the peaks almost disappeared. In contrast, although the signal

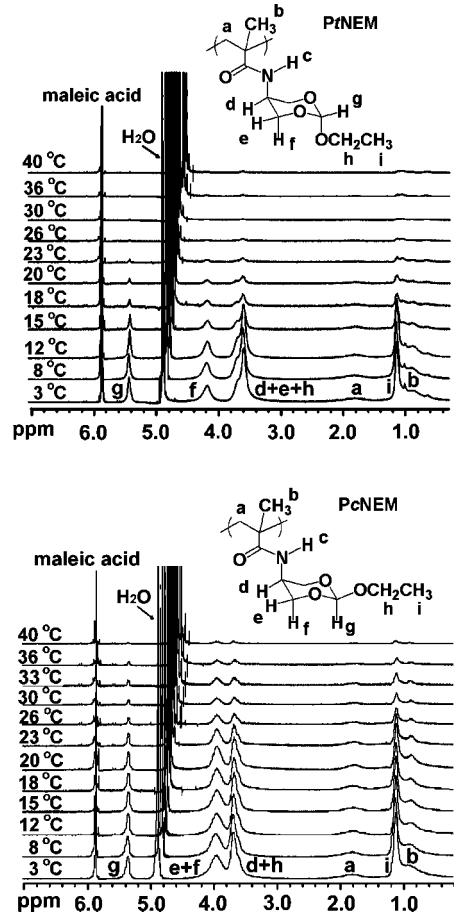

Figure 6. Temperature-dependent ^{1}H NMR spectra of P*t*NEM and P*c*NEM in the deuterated phosphate buffer (10 mM, pD 8.4).

intensities of P*c*NEM decreased noticeably with the increase in temperature, the peaks were clearly observable even at 33 °C, a temperature of ca. 11 °C above its CP. On the basis of the DSC and ^{1}H NMR results, it can be deduced that P*c*NEM underwent a liquid−liquid phase separation accompanied by the formation of coacervate droplets while P*t*NEM likely exhibited a liquid−solid phase transition in the heating process.[6a,24b] This speculation was supported by the microscopic observations of the polymer solutions (Figure S10). Above their CPs, clear coacervate droplets were formed in the P*c*NEM aqueous solution while solidlike precipitates were observed for P*t*NEM. This drastic difference in dehydration behaviors of the polymers above their CPs could be ascribed to the fact that the *trans* configuration of the pendant cyclic groups enabled P*t*NEM chains to pack densely, thus leading to the more efficient dehydration and a larger ΔH. In addition, the lower CP of P*t*NEM might also be accounted for by the ease of densely packing of the polymer chains. Further experiments revealed that molecular weights of the polymers show a little effect on their LCSTs but did not affect their transition enthalpies very much (Table 1 and Table S1).

Figure 7 shows the temperature dependence of the I_1/I_3 ratio of Py in the P*t*NEM and P*c*NEM aqueous solutions. At very low concentration (1.0 μg/mL), the ratio was ca. 1.8 in both polymer solutions and did not change much within the tested temperature. This value is identical with that measured in water, implying that Py resided mostly in the bulk water. At higher polymer concentrations, different fluorescence results were obtained. For P*t*NEM below its cac, the ratio decreased abruptly around its LCST with the temperature increase, indicating the transfer of Py into the collapsed polymer-rich phase. This decrease in I_1/I_3 ratio was consistent with that for PNIPAM in

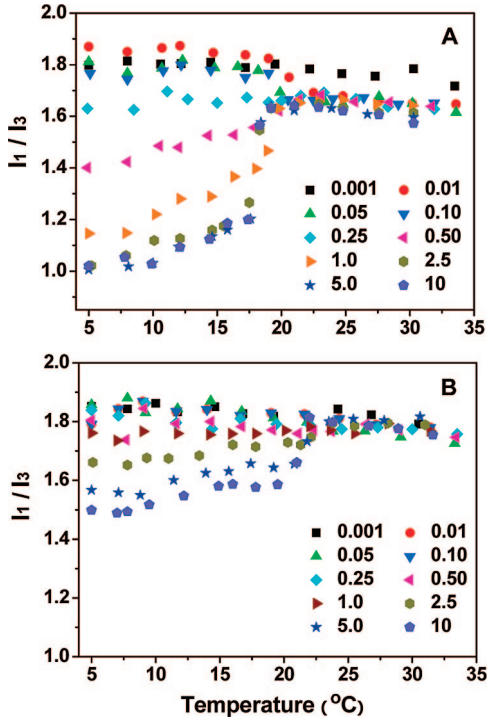

Figure 7. Temperature-dependent changes in I_1/I_3 ratio of pyrene in P*t*NEM (A) and P*c*NEM (B) aqueous solutions (10 mM pH 8.4 phosphate buffer) at various polymer concentrations (mg/mL).

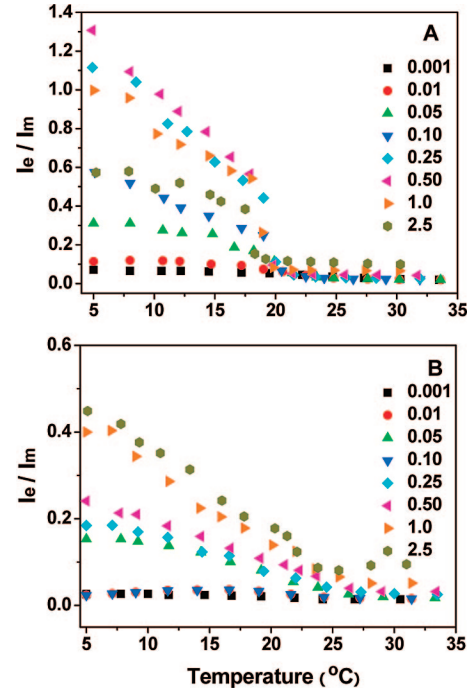

Figure 8. Temperature-dependent changes in I_e/I_m ratio of pyrene in P*t*NEM (A) and P*c*NEM (B) aqueous solutions (10 mM pH 8.4 phosphate buffer) at various polymer concentrations (mg/mL).

water.[8a,26] By contrast, at concentrations above the cac, the I_1/I_3 ratio showed a sharp increase as the temperature was raised through the LCST, demonstrating that the polarity of the microenvironments sensed by Py increased. A similar phenomenon was also reported for some hydrophobically modified PNIPAM derivatives.[8a,26a,27] As aforementioned, although P*t*NEM seems not a typical amphiphilic polymer, it did form some kind of aggregates above its cac, and there were some hydrophobic microdomains that can solvate Py below its LCST. Upon heating through the LCST, dehydration of the polymer chains may cause the structural deformation of the original microdomains, resulting in the newly formed polymer-rich aggregates that can still solvate Py molecules but were more polar in nature. In the case of P*c*NEM above its cac, the I_1/I_3 ratio also demonstrated an abrupt increase at its LCST. However, no clear change in I_1/I_3 was observed below the cac within the measured temperature range. In addition, the I_1/I_3 ratios in P*c*NEM solution were larger than those in P*t*NEM above their respective LCSTs, which suggests that the former was less dehydrated than the latter above their respective LCSTs. This result is well agreed with those obtained from the ^{1}H NMR and DSC measurements.

The influence of temperature on the excimer formation of Py in the polymer solutions was also studied. Figure 8 shows the changes in I_e/I_m as a function of temperature. In aqueous solutions of both P*t*NEM and P*c*NEM, Py excimers were formed at appropriate polymer concentrations, and the values of I_e/I_m gradually decreased with increasing the temperature until their respective LCSTs. This can be ascribed to the thermally induced nonradiative decaying of the excimers. In the case of P*t*NEM, I_e/I_m showed an abrupt decrease as the temperature was raised through the LCST, beyond which no clear excimer emission was observed. This observation is consistent with the temperature-dependent fluorescence behaviors of the Py-modified PNIPAM in aqueous solution[26b,28] and can be attributed to the redistribution of Py molecules from the original microdomains (below the LCST) to the newly formed polymer-rich aggregates (above the LCST). This assumption was also supported by the temperature-dependent emission spectra of Py in the polymer solutions (Figure S11). The Py monomer emission showed an abrupt increase at the LCST while the excimer emission sharply decreased, indicating a drastic change of Py molecules from an aggregated state to a diluted and separated distribution.

pH-Dependent Hydrolysis. As previously reported, the unique feature of the present thermoresponsive polymers is their acid sensitivity.[15a] The acid-catalyzed hydrolyses of P*t*NEM and P*c*NEM in the deuterated acetate buffers (pD 5.0) were first evaluated by ^{1}H NMR measurements (Figure 9). It can be seen that at the starting point no or only very weak proton peaks were observed. The polymers were gradually dissolved with prolonging the hydrolysis time and became completely soluble at ca. 140 min. P*t*NEM hydrolyzed almost completely within 260 min. The hydrolysis of P*c*NEM was slower; the proton signals (peak g) assigned to the cyclic orthoester group was still observed after 300 min. Furthermore, the hydrolysis products of the two polymers were different. There are two types of units in the completely hydrolyzed polymer chains: one with two hydroxyl groups (unit I) and the other one with a hydroxyl group and a formate group (unit II in Scheme 2). By comparing the intensities of peaks d′ and d″, it can be seen that the contents of the two units were almost equal for the hydrolyzed P*t*NEM whereas P*c*NEM produced much more units with two hydroxyl groups (unit I), which can be attributed to the difference in the configurations of the pendant cyclic groups. As shown in Scheme 3, hydrolysis of the cyclic orthoester is believed to proceed mainly through two competing paths: the endocyclic ring cleavage (path A) and the breaking of the exocyclic ethoxy group (path B).[29] Path A produces the hydrolysis products with both unit I and unit II while in the path B only unit II can be obtained. Our present ^{1}H NMR results demonstrated that path A dominated the hydrolysis mechanism of P*c*NEM while the hydrolysis of P*t*NEM, in some extent, took place through path B. Dory et al. reported that the hydrolysis processes of cyclic orthoesters were affected by the stereoelectronic effects and the steric factors.[29a] The conformational structures of the pendant cyclic orthoester moieties in the polymers are expected to influence the hydrolysis rate as well as the hydrolysis products.

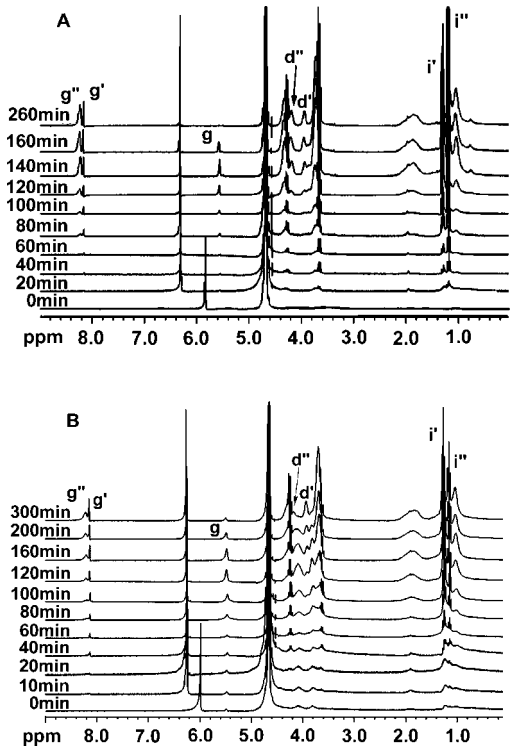

Figure 9. ^{1}H NMR spectra of P*t*NEM (A) and P*c*NEM (B) in the deuterated acetate buffer at different hydrolysis times. pD ca. 5.0, 37 °C, polymer concentration: 5.0 mg/mL.

Scheme 2

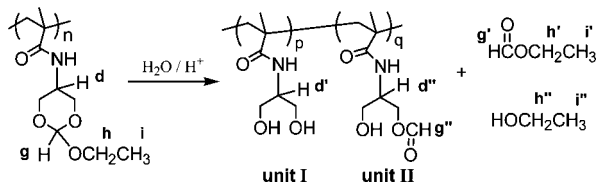

Scheme 3. Hydrolysis Paths of the Pendant Cyclic Orthoester Moieties

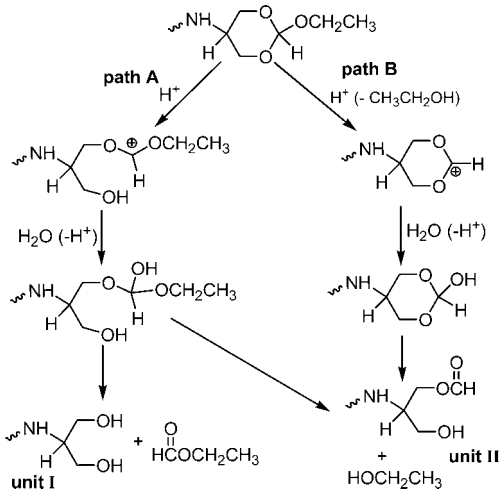

We attempted to clarify the predominant conformations of the orthoester moieties by NOESY of ^{1}H NMR but did not obtain clear and convinced results (data not shown).

The pH-dependent hydrolyses of P*t*NEM and P*c*NEM were further demonstrated by monitoring the changes in the transmittance of their aqueous solutions with different pH values at 37 °C (Figure 10). It can be seen that the turbid polymer solutions

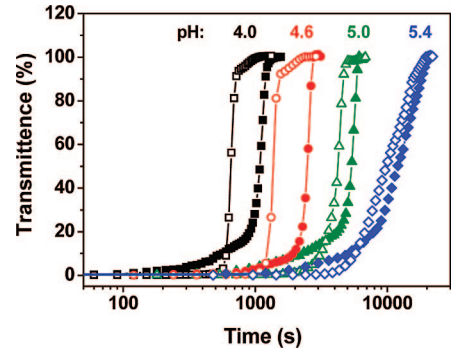

Figure 10. Transmittance vs hydrolysis time plots of P*t*NEM (solid symbol) and P*c*NEM (empty symbol) in buffer solutions of various pHs at 37 °C, λ = 500 nm, 1.0 mg/mL.

became clear at specific times, indicating that the polymers were dissolved in water due to the partial hydrolysis of the pendant orthoester groups. The time for the polymer solutions to become transparent (95% transmittance) was reduced with the decrease in pH, indicating that the polymers were sensitive to an acidic environment. At the same pH, the time for P*c*NEM solution to become transparent is shorter than that for P*t*NEM, which can be attributed to the more polar character of P*c*NEM above its LCST as well as the more hydroxyl groups in the partially hydrolyzed polymer chains.

Conclusion

We demonstrate that the *trans* and *cis* configurations of the pendant cyclic groups have significant effects on the aqueous solution properties of P*t*NEM and P*c*NEM as well as their hydrolysis behavior. Both polymers show reversible and sensitive thermoresponsive behaviors at certain temperatures. P*c*NEM shows a higher CP with a smaller transition enthalpy compared to P*t*NEM. It is confirmed that P*c*NEM exhibits a liquid−liquid phase separation while P*t*NEM displays a liquid−solid phase transition around their respective CPs. These two polymers can form some kind of aggregates even below their respective CPs. P*t*NEM tends to form more hydrophobic microdomains with a lower cac. Above the LCSTs, the polymer-rich phase of P*c*NEM is more polar than that of P*t*NEM. In addition, the two polymers show the pH-dependent hydrolysis behaviors, and their CPs can be tuned by controlling the hydrolysis under mildly acidic conditions. We expect that P*t*NEM and P*c*NEM and their related copolymers possess great potential for tumor tissue and/or intracellular drug delivery. For example, block copolymers consisting PEG segment and P*t*NEM block may form micellar structures at 37 °C which can be used as hydrophobic drug carriers.

Acknowledgment. This work was financially supported by the National Natural Science Foundation of China (No. 20474005 and 50673004). The authors thank Prof. Zheming Wang for his kind help in X-ray diffraction measurements and Prof. Yuguo Ma for his kind help in the manuscript preparation.

Supporting Information Available: NMR spectra of the monomers and their polymers, crystal structures of the monomers, DLS results, micrographs, more emission and excitation spectra, and thermosensitive properties of the polymers with different molecular weights. This material is available free of charge via the Internet at http://pubs.acs.org.

References and Notes

(1) (a) Schmaljohann, D. *Adv. Drug Delivery Rev.* **2006**, *58*, 1655–1670.
(b) Gil, E. S.; Hudson, S. A. *Prog. Polym. Sci.* **2004**, *29*, 1173–1222.

(2) (a) Lu, Y.; Mei, Y.; Drechsler, M.; Ballauff, M. *Angew. Chem., Int. Ed.* **2006**, *45*, 813–816. (b) Meyer, D. E.; Shin, B. C.; Kong, G. A.; Dewhirst, M. W.; Chilkoti, A. *J. Controlled Release* **2001**, *74*, 213–224. (c) Hinrichs, W. L. J.; Schuurmans-Nieuwenbroek, N. M. E.; van de Wetering, P.; Hennink, W. E. *J. Controlled Release* **1999**, *60*, 249–259. (d) Carter, S.; Rimmer, S.; Rutkaite, R.; Swanson, L.; Fairclough, J. P. A.; Sturdy, A.; Webb, M. *Biomacromolecules* **2006**, *7*, 1124–1130. (e) Kikuchi, A.; Okuhara, M.; Karikusa, F.; Sakurai, Y.; Okano, T. *J. Biomater. Sci., Polym. Ed.* **1998**, *9*, 1331–1348. (f) Schild, H. G. *Prog. Polym. Sci.* **1992**, *17*, 163–249.

(3) (a) Ohya, Y.; Toyohara, M.; Sasakawa, M.; Arimura, H.; Ouchi, T. *Macromol. Biosci.* **2005**, *5*, 273–276. (b) Tachibana, Y.; Kurisawa, M.; Uyama, H.; Kakuchi, T.; Kobayashi, S. *Chem. Commun.* **2003**, 106–107. (c) Jia, Z. F.; Chen, H.; Zhu, X. Y.; Yan, D. *J. Am. Chem. Soc.* **2006**, *128*, 8144–8145. (d) Shimokuri, T.; Kaneko, T.; Serizawa, T.; Akashi, M. *Macromol. Biosci.* **2004**, *4*, 407–411. (e) Meyer, D. E.; Chilkoti, A. *Nat. Biotechnol.* **1999**, *17*, 1112–1115.

(4) (a) Taylor, L. D.; Cerankowski, L. D. *J. Polym. Sci., Part A: Polym. Chem.* **1975**, *13*, 2551–2570. (b) Feil, H.; Bae, Y. H.; Feijen, J.; Kim, S. W. *Macromolecules* **1993**, *26*, 2496–2500.

(5) (a) Lutz, J.-F.; Hoth, A. *Macromolecules* **2006**, *39*, 893–896. (b) Barker, I. C.; Cowie, J. M. G.; Huckerby, T. N.; Shaw, D. A.; Soutar, I.; Swanson, L. *Macromolecules* **2003**, *36*, 7765–7770. (c) Suwa, K.; Morishita, K.; Kishida, A.; Akashi, M. *J. Polym. Sci., Part A: Polym. Chem.* **1997**, *35*, 3087–3094. (d) Nichifor, M.; Zhu, X. X. *Polymer* **2003**, *44*, 3053–3060.

(6) (a) Sugihara, S.; Kanaoka, S.; Aoshima, S. *Macromolecules* **2004**, *37*, 1711–1719. (b) Park, J. S.; Kataoka, K. *Macromolecules* **2007**, *40*, 3599–3609.

(7) (a) Xia, Y.; Burke, N. A. D.; Stover, H. D. H. *Macromolecules* **2006**, *39*, 2275–2283. (b) Furyk, S.; Zhang, Y. J.; Ortiz-Acosta, D.; Cremer, P. S.; Bergbreiter, D. E. *J. Polym. Sci., Part A: Polym. Chem.* **2006**, *44*, 1492–1501.

(8) (a) Chung, J. E.; Yokoyama, M.; Suzuki, K.; Aoyagi, T.; Sakurai, Y.; Okano, T. *Colloids Surf., B* **1997**, *9*, 37–48. (b) Duan, Q.; Miura, Y.; Narumi, A.; Shen, X. D.; Sato, S.; Satoh, T.; Kakuchi, T. *J. Polym. Sci., Part A: Polym. Chem.* **2006**, *44*, 1117–1124. (c) Mori, T.; Shiota, Y.; Minagawa, K.; Tanaka, M. *J. Polym. Sci., Part A: Polym. Chem.* **2005**, *43*, 1007–1013.

(9) (a) Haba, Y.; Kojima, C.; Harada, A.; Kono, K. *Angew. Chem., Int. Ed.* **2007**, *46*, 234–237. (b) Carter, S.; Hunt, B.; Rimmer, S. *Macromolecules* **2005**, *38*, 4595–4603. (c) Xu, J.; Ye, J.; Liu, S. Y. *Macromolecules* **2007**, *40*, 9103–9110.

(10) Freitag, R.; Garret-Flaudy, F. *Langmuir* **2002**, *18*, 3434–3440.

(11) Aoki, T.; Muramatsu, M.; Torii, T.; Sanui, K.; Ogata, N. *Macromolecules* **2001**, *34*, 3118–3119.

(12) (a) Baltes, T.; Garret-Flaudy, F.; Freitag, R. *J. Polym. Sci., Part A: Polym. Chem.* **1999**, *37*, 2977–2989. (b) Hietala, S.; Nuopponen, M.; Kalliomaki, K.; Tenhu, H. *Macromolecules* **2008**, *41*, 2627–2631.

(13) (a) Shim, W. S.; Kim, S. W.; Lee, D. S. *Biomacromolecules* **2006**, *7*, 1935–1941. (b) Yin, X. C.; Hoffman, A. S.; Stayton, P. S. *Biomacromolecules* **2006**, *7*, 1381–1385. (c) Soppimath, K. S.; Tan, D. C.-W.; Yang, Y. Y. *Adv. Mater.* **2005**, *17*, 318–323.

(14) (a) Yin, X. C.; Stover, H. D. H. *Macromolecules* **2002**, *35*, 10178–10181. (b) Ihata, O.; Kayaki, Y.; Ikariya, T. *Chem. Commun.* **2005**, 2268–2270.

(15) (a) Huang, X. N.; Du, F. S.; Ju, R.; Li, Z. C. *Macromol. Rapid Commun.* **2007**, *28*, 597–603. (b) Huang, X. N.; Du, F. S.; Zhang, B.; Zhao, J. Y.; Li, Z. C. *J. Polym. Sci., Part A: Polym. Chem.* **2008**, *46*, 4332–4343.

(16) (a) Cui, Z. W.; Lee, B. H.; Vernon, B. *Biomacromolecules* **2007**, *8*, 1280–1286. (b) Cho, J. Y.; Sohn, Y. S.; Gutowska, A.; Jeong, B. *Macromol. Rapid Commun.* **2004**, *25*, 964–967. (c) Neradovic, D.; van Nostrum, C. F.; Hennink, W. E. *Macromolecules* **2001**, *34*, 7589–7591.

(17) Gillies, E. R.; Frechet, J. M. *J. Bioconjugate Chem.* **2005**, *16*, 361–368.

(18) Stempel, G. H.; Cross, R. P.; Mariella, R. P. *J. Am. Chem. Soc.* **1950**, *72*, 2299–2300.

(19) (a) Kalyanasundaram, K.; Thomas, J. K. *J. Am. Chem. Soc.* **1977**, *99*, 2039–2044. (b) Winnik, F. M. *Chem. Rev.* **1993**, *93*, 587–614.

(20) Zana, R.; Guveli, D. *J. Phys. Chem.* **1985**, *89*, 1687–1690.

(21) Noda, T.; Hashidzume, A.; Morishima, Y. *Macromolecules* **2000**, *33*, 3694–3704.

(22) Kim, J. H.; Domach, M. M.; Tilton, R. D. *Colloids Surf., A* **1999**, *150*, 55–68.

(23) (a) Winnik, F. M. *Macromolecules* **1990**, *23*, 233–242. (b) Oyama, H. T.; Hemker, D. J.; Frank, C. W. *Macromolecules* **1989**, *22*, 1255–1260.

(24) (a) Yin, X. C.; Stolver, H. D. H. *Macromolecules* **2005**, *38*, 2109–2115. (b) Maeda, T.; Kanda, T.; Yonekura, Y.; Yamamoto, K.; Aoyagi, T. *Biomacromolecules* **2006**, *7*, 545–549. (c) Yamamoto, K.; Serizawa, T.; Akashi, M. *Macromol. Chem. Phys.* **2003**, *204*, 1027–1033.

(25) (a) Cheng, H.; Shen, L.; Wu, C. *Macromolecules* **2006**, *39*, 2325–2329. (b) Ding, Y. W.; Ye, X. D.; Zhang, G. Z. *Macromolecules* **2005**, *38*, 904–908.

(26) (a) Schild, H. G.; Tirrell, D. A. *Langmuir* **1991**, *7*, 1319–1324. (b) Ringsdorf, H.; Venzmer, J.; Winnik, F. M. *Macromolecules* **1991**, *24*, 1678–1686.

(27) Cao, Z. Q.; Liu, W. G.; Gao, P.; Yao, K. D.; Li, H. X.; Wang, G. H. *Polymer* **2005**, *46*, 5268–5277.

(28) Laukkanen, A.; Winnik, F. M.; Tenhu, H. *Macromolecules* **2005**, *38*, 2439–2448.

(29) (a) Li, S.; Dory, Y. L.; Deslongchamps, P. *Tetrahedron* **1996**, *52*, 14841–14854. (b) By, K.; Nantz, M. H. *Angew. Chem., Int. Ed.* **2004**, *43*, 1117–1120.

MA800783V